

Polyethylene Flame Retarded with Expandable Graphite and a Novel Intumescent Additive

Walter Wilhelm Focke,¹ Hermanus Joachim Kruger,¹ Washington Mhike,¹ Albertus Taute,¹ Albert Roberson,¹ Osei Ofosu²

¹SARChI Chair in Carbon Technology and Materials, Institute of Applied Materials, Department of Chemical Engineering, University of Pretoria, Private Bag X20, Hatfield 0028, South Africa

²CSIR Materials Science and Manufacturing, PO Box 1124, Port Elizabeth 6000, South Africa

Correspondence to: W.W. Focke (E-mail: walter.focke@up.ac.za)

ABSTRACT: A novel intumescent additive was synthesized by neutralizing 3,5-diaminobenzoic acid hydrochloride salt with ammonium dihydrogen phosphate. This compound, which melts at 257°C, decomposes concurrently to release carbon dioxide gas. The flame retardant performance of this compound as a primary fire retardant and in combination with expandable graphite (EG) was evaluated by cone calorimetry. Cone calorimeter results showed that addition of 10 wt % EG alone lowers peak heat release rate (pHRR) of carbon black-pigmented polyethylene from 710 ± 109 to 342 ± 15 kW m⁻², whereas addition of 27 wt % of the novel intumescent lowered it to 400 ± 16 kW m⁻². Combinations of these two additives were able to decrease the pHRR even further. Furthermore, the novel intumescent additive reduced the flame out time from 773 ± 307 to 537 ± 69 s although all other EG containing samples increased it. © 2014 Wiley Periodicals, Inc. *J. Appl. Polym. Sci.* **2014**, *131*, 40493.

KEYWORDS: flame retardance; polyolefins; composites; graphite

Received 4 October 2013; accepted 19 January 2014

DOI: 10.1002/app.40493

INTRODUCTION

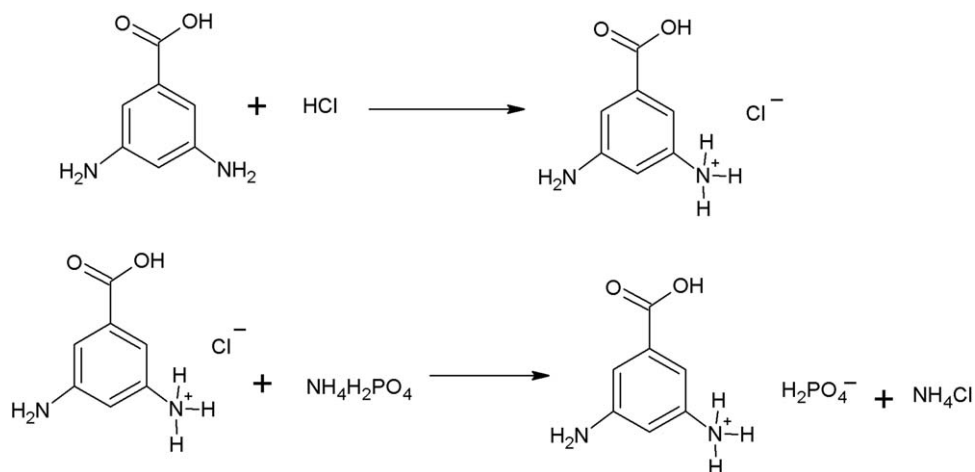
Polyethylenes are a family of commodity polymers (HDPE, LDPE, and LLDPE) primarily used as packaging materials. They are also used to fabricate moulded products such as battery boxes, air conditioning ducting, pipes, and cable sheathing. Polyethylenes feature high heats of combustion and have a low propensity for char formation.¹ As a result, these products present a potential fire hazard in certain applications, for example, deep-level underground mining. Cone calorimetry presents a modern method for measuring the ignition time, heat release rate (HRR), combustion products, and other flammability characteristics of polymer samples. This fire testing instrument determines the transient HRR by measuring transient oxygen consumption rate in the exhaust gases. According to Babrauskas and Peacock² the HRR is the most important single variable in characterizing the “flammability” of products and thus the fire hazard they may pose. Among the more widely used polymers, pure polyethylenes feature the highest heat release capacities and the highest HRRs in cone calorimeter tests.³

It is therefore necessary, for critical applications, to flame retard polyethylene products with flame retardant additives. A wide range of effective additives are available.^{1,3} Recent studies have highlighted the utility of expandable graphite (EG), intumescent

flame retardants, and their synergistic combinations, which improve the fire behavior of polyethylene.^{1,4-9} Intumescent additives cause the materials to swell when exposed to fire or heat to form a carbonaceous foam residue that acts as a heat insulator and a physical barrier to the transport of oxygen and pyrolysis products.^{3,10-12}

EG is actually a partially oxidized, intercalated form of graphite containing intercalated guest species (e.g., sulfuric acid anions) in between the stacked graphene layers.^{13,14} A key property of EG is its tendency to exfoliate explosively, that is, expand rapidly in a worm-like manner when heated to high temperatures.¹⁵⁻¹⁷ When this occurs at the surface of a polymer, the low density vermicular graphite that is formed provides a protective barrier similar to that generated by conventional intumescent additives.

According to Han et al.⁹ and Xie and Qu⁵ better fire properties are possible with combinations of EG and other intumescent flame retardants. Despite this, only a few such combinations have been explored to date. Therefore this communication reports on the synthesis and characterization of a novel intumescent flame retardant additive for use as a primary intumescent flame retardant and in combination with an EG. The unique aspect of these two additives is that they both feature



Scheme 1. Synthesis of the phosphate salt of 3,5-diaminobenzoic acid.

relatively high thermal stabilities. This could make them useful in applications where the polymer conversion requires high processing temperatures, for example, rotomoulding. The fire performance of these additives, on their own and in combinations, in polyethylene was studied using cone calorimeter fire testing.

EXPERIMENTAL

Materials

The chemicals 3,5-diamino benzoic acid (DABA) [535-87-5], ammonium dihydrogen phosphate [7722-76-1], and hydrochloric acid [7647-01-0] were sourced from Sigma-Aldrich, Protea Chemicals and Merck, respectively. Sasol Polymers supplied the low density polyethylene in powder and pellet form. It was injection moulding grade LT019 with density 0.919 g cm^{-3} and MFI 20.5 g/10 min at $190^\circ\text{C}/2.16 \text{ kg}$. Carbon black grade N660 was sourced from Ferro Industrial Products. The EG grade ES170 300A, with a high expansion onset temperature, was sourced from Qingdao Kropfmuehl, China. The d_{10} , d_{50} , and d_{90} particle sizes were 313, 533, and 807 μm , respectively (Mastersizer Hydroliser 2000, Malvern Instruments, Malvern, UK). The density was $2.23 \pm 0.01 \text{ g cm}^{-3}$ and the surface area in the pre-expanded form was $0.66 \text{ m}^2 \text{ g}^{-1}$ (Nova 1000e BET in N_2 at 77 K).

Synthesis of Phosphate Salt of DABA

Scheme 1 shows the reaction details. The synthesis procedure was as follows: seven moles of DABA (1065 g) was weighed out into a large glass container placed in an ice bath, which contained about 500 g crushed ice. Seven ampules of concentrated hydrochloric acid (containing 1 mol HCl each) were added drop wise to the DABA container, which was continuously stirred and maintained at a temperature below ambient. At this stage the solution developed a dark brown colour, most likely due to oxidation of a minor portion of the DABA. Next, seven moles (805 g) ammonium dihydrogen phosphate powder was added slowly to the reaction mixture with continued stirring. During this procedure, the colour of the liquid phase changed from brown to orange. The final pH was 7.8. The precipitated silver-white crystals were recovered using vacuum filtration. The filter cake was first washed with distilled water and then with

acetone. The resulting filter cake was oven dried at 50°C for 12 h and milled into a fine powder. The yield was 95%.

Preparation of the Polyethylene Compounds

Polyethylene compounds containing EG and/or phosphate salt of DABA (DABAP) were compounded on a 28 mm co-rotating intermeshing twin screw laboratory extruder ($L/D = 16$) at a screw speed of 140–220 rpm. The compounder's screw design comprised intermeshing kneader elements with a forward transport action. The four extrusion processing stage temperatures, feed to die, were set at 120, 175, 175, and 180°C , respectively. The extruded strands were granulated and pressed into flat sheets in a hot press set at 180°C . The final sheet dimensions were $100 \times 100 \text{ mm} \times 3.2 \pm 0.1 \text{ mm}$. A polyethylene compound containing 3 wt % carbon-black (N660) was prepared in a similar way. This compound was used as the reference sample for cone calorimeter testing. The compound containing 27 wt % DABAP also contained 3 wt % carbon-black. This maintained a consistent range of dark product sheets as delivered for all EG containing compounds, to ensure comparable heat absorption during cone calorimeter testing.

Characterization and Analysis

Fourier-Transform Infrared Spectroscopy (FTIR) spectra were recorded on a Perkin Elmer Spectrum RX FT-IR, coupled with a computer using Spectrum v5.0.1 software, with a scan resolution of 2.0 cm^{-1} . A total of 32 interferograms were collected for each sample applying single beam radiation in an ATR configuration.

The compositions of the graphite particles and the DABAP were determined by X-ray fluorescence (XRF) analysis performed using a wavelength-dispersive spectrometer (ARL 9400XP+ XRF). The samples were prepared as pressed powder briquettes and introduced to the spectrometer. The powders were ground in a tungsten carbide milling vessel and roasted at 1000°C for determination of the loss on ignition (LOI).

Scanning Electron Microscopic (SEM) images were obtained using an ultrahigh resolution field emission SEM (HR FEGSEM Zeiss Ultra Plus 55) with an InLens detector at acceleration voltages of as low as 1 kV to ensure maximum resolution of

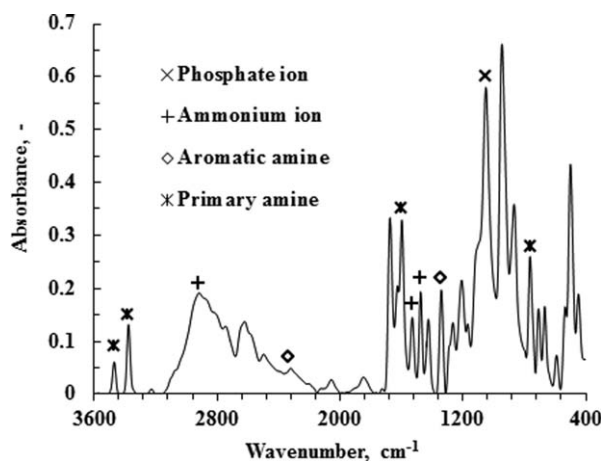


Figure 1. FTIR spectrum for 3,5-diaminobenzoic acid phosphate (DABAP).

surface detail. No electro-conductive coating was applied on the graphite particles.

Thermal Analysis

Differential scanning calorimetry data were obtained on a Perkin Elmer PYRIS Diamond DSC. The temperature was scanned from 30 to 370°C at a scan rate of 10°C min⁻¹ with nitrogen flowing at a rate of 50 mL min⁻¹.

Thermogravimetric analysis (TGA) was performed using the dynamic method on a TA Instruments SDT Q600 instrument. About 7 mg of sample was placed in a 50 μ L alumina pan with an alumina lid. Temperature was scanned from 50 to 900°C at a scan rate of 10°C min⁻¹ with gas flowing at a rate of 50 mL min⁻¹.

Thermal expansion measurements were conducted on a TA instruments Q400 Thermo Mechanical Analyzer. Sufficient EG powder was placed in an alumina sample pan such that the bed height was between 35 and 40 μ m. The flake expansion behavior was measured with a flat-tipped standard expansion probe using an applied force of 0.02 N. The temperature was scanned from 30 to 1000°C at a scan rate of 10°C min⁻¹ in a nitrogen atmosphere. The expansion relative to the original powder bed height was reported. The same procedure was used to determine the softening point of the DABAP using a thin tipped penetration probe. In this case however, the applied force was 0.01 N, the temperature was scanned from 30 to 500°C at a scan rate of 4°C min⁻¹ and the starting sample height was 229 μ m.

Cone Calorimeter Flammability Testing

The ISO 5660-1 standard was followed in performing the cone calorimeter tests using a Dual Cone Calorimeter (Fire Testing

Technology (UK)). Three specimens of each composition were tested and average values are reported. The sheet dimensions were 100 \times 100 \times 3.2 mm. They were placed horizontally on aluminium foil and exposed perpendicularly from above to an external heat flux of 35 kW m⁻².

RESULTS AND DISCUSSION

Characterization

The synthesis yielded the DABAP as shown by the reactions of Scheme 1. It is expected that one of the amine functional groups of DABA became protonated by the phosphoric acid while the other remained a free amine (that nevertheless participates in hydrogen bonding). The FTIR spectrum shown in Figure 1 is consistent with these assertions. The presence of a free primary aromatic amine is supported by the following absorption peaks in the FTIR spectrum¹⁸: The two bands located at 3469 and 3377 cm⁻¹ are characteristic of the N—H stretching vibrations in primary amines. The sharp band at 1600 is due to the N—H bending vibration in primary amines. The band at 1340 cm⁻¹ is characteristic of the C—N stretch of aromatic amines. Finally, the sharp peak at 763 cm⁻¹ is consistent with the N—H wagging vibration of primary amines. The band at 1050 cm⁻¹ is attributed to the phosphate ion. The broad band with a peak at 2917 cm⁻¹ is consistent with the presence of a primary ammonium ion (N—H stretch). The primary ammonium ion N—H bending vibrations are indicated by the two bands located at 1530 and 1475 cm⁻¹.

Table I reports the XRF results for DABAP and the EG. According to the XRF results, the apparent P₂O₅ content of DABAP is 25.47% whereas the expected, that is, theoretical value is 28.37%. The chlorine content suggests co-crystallization of the chloride salt of DABA. Both samples contain some inorganic impurities. In DABAP the source is probably the technical grade ammonium dihydrogen phosphate that was used. The EG contains intercalated sulphuric acid moieties and as expected the XRF results showed the presence of a significant amount of sulphur. However, the graphite sample also contains other inorganic impurities. The main impurity elements were silicon and aluminium suggesting that the precursor graphite may have been contaminated with clay minerals.

The SEM micrograph in Figure 2 shows the morphology of the DABAP crystals. The EG particles also have a flake-like nature but the flakes are much larger.

Thermal Analysis

Figure 3 shows the TGA mass loss curve and the differential mass loss (DTG) curves for DABAP obtained in N₂, together

Table I. XRF Results with Composition Indicated as wt %

ES170 300A	SiO ₂	TiO ₂	Al ₂ O ₃	Fe ₂ O ₃	MnO	MgO	CaO
	1.06	0.02	0.63	0.10	0.03	0.16	1.58
	Na ₂ O	K ₂ O	SO ₃	Co ₃ O ₄	S	Rest	
	0.48	0.07	6.06	<0.01	<0.01	89.67	
DABAP	Fe ₂ O ₃	MgO	Na ₂ O	P ₂ O ₅	SO ₃	Cl	Rest
	0.05	0.04	0.29	25.47	0.02	0.68	73.46

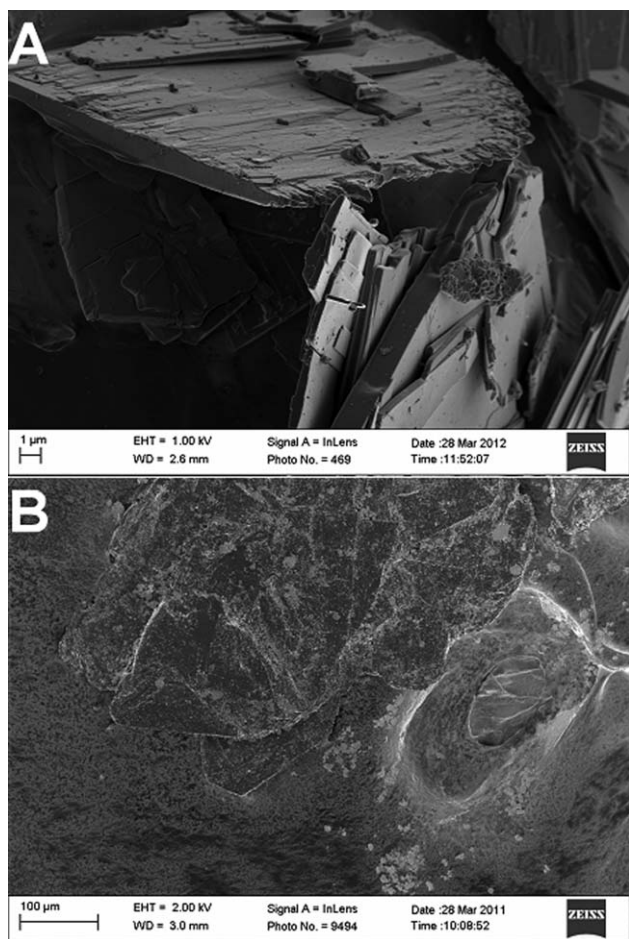


Figure 2. SEM micrographs of (A) 3,5-diaminobenzoic acid phosphate crystals and (B) expandable graphite flakes.

with the TGA trace for the EG obtained in nitrogen and air. The mass loss for the EG in air occurs in two steps. The first corresponds to the gas released during the exfoliation event and this one is also observed in a nitrogen atmosphere. The mass loss in air and nitrogen at 600°C amount to 10 and 7 wt %, respectively. The second corresponds to the oxidation of graphite residue. The mass loss for the DAPAB occurs in four steps. The minor mass loss (1.17%) below 200°C probably reflects the loss of moisture. Thereafter a steep mass loss (ca. 15.5%) event occurs with an onset temperature of 254°C. This probably reflects the loss of CO₂ due to the decarboxylation of the DABAP. The theoretical mass loss for decarboxylation is 17.6%. Mass loss continues and next reaches a peak value at a temperature of 446°C. We attribute this to the char-forming decomposition reaction that also releases ammonia gas. The pyrolysis of the char that is formed continues as the temperature is raised. It reaches a maximum rate at 860°C. At 900°C, the carbonized char residue that remains represents just above 27% of the initial DABAP mass.

Figure 4 shows the differential thermal analysis (DTA) curves together with the TGA trace for DABAP. It is clear from this figure that all the mass loss events seen in the TGA are associated with endothermic events. The DSC scan in Figure 5

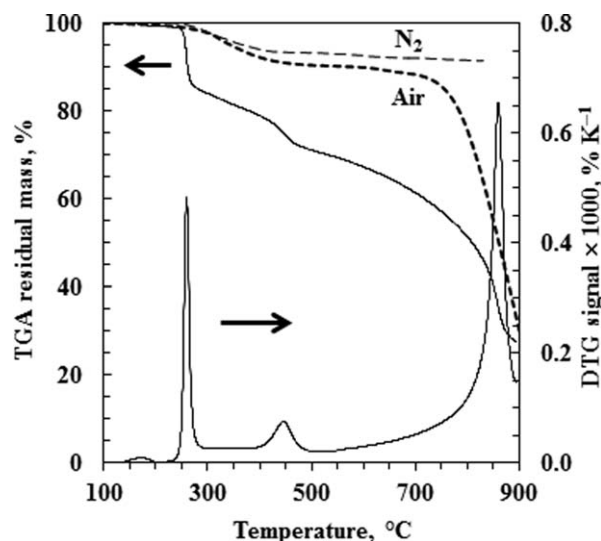


Figure 3. TGA and DTG curves for DABAP obtained in N₂ and TGA traces for the expandable graphite in air and in nitrogen (dotted lines). Temperature was scanned from 25 to 900°C at a scan rate of 10°C min⁻¹ with gas flowing at a rate of 50 mL min⁻¹.

indicates a sharp endothermic peak with an onset temperature of 257°C. The shape and the corresponding enthalpy change of 624 kJ kg⁻¹ are reminiscent of a melting event. Indeed, the thermal mechanical analysis (TMA) curve in Figure 5 indicates softening of the material at this temperature. In conclusion, the melting of DABAP commences with simultaneously thermal decomposition at about 257°C.

The key property of EG in fire retardant applications is the ability to exfoliate within a narrow temperature range. Figure 6 compares the TMA expansion performance of the EG sample with the behavior of DABAP. The exfoliation onset temperature of the EG was about 300°C. It is clear that the DABAP softened well before the onset of the EG expansion, which promotes expansion of EG through DABAP thus increasing the thermal barrier thickness.

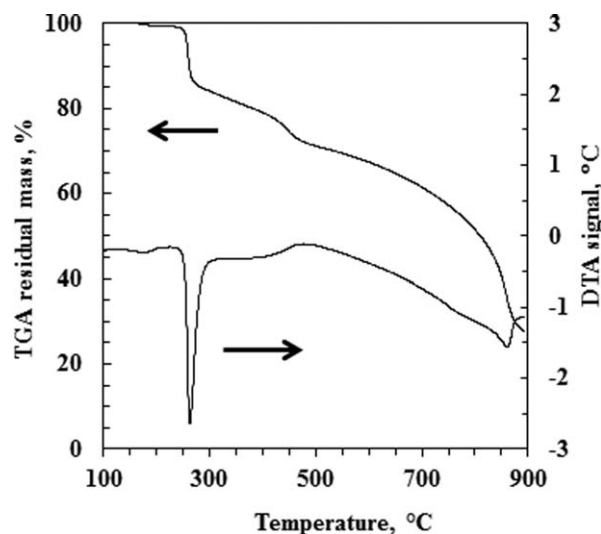


Figure 4. TGA and DTA curves for DABAP obtained at a scan rate of 10°C min⁻¹ with N₂ gas flowing at a rate of 50 mL min⁻¹.

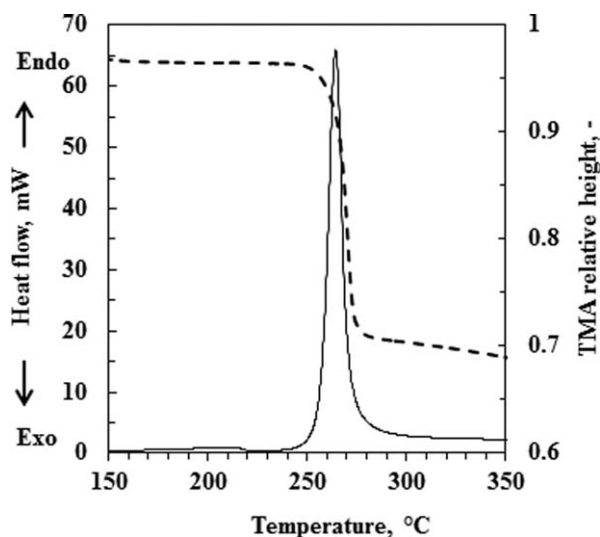


Figure 5. DSC and TMA curves for DABAP obtained with N_2 gas flowing at a rate of 50 mL min^{-1} . The temperature scan rates were $10^\circ\text{C min}^{-1}$ and 4°C min^{-1} , respectively.

Flammability

The cone calorimeter results are presented in Figures 7–13 and are summarized in Table II. Figure 7 shows representative HRR curves obtained from the cone calorimeter tests. Figures 8 reports average values for the total heat released and the peak heat release rates (pHRRs). Unexpectedly the total heat release value measured was lowest for the carbon black-pigmented polyethylene, hereafter referred to as neat polyethylene (Table II). It was $90 \pm 18 \text{ MJ m}^{-2}$ for the neat polyethylene and $130 \pm 6 \text{ MJ m}^{-2}$ for the compound with 27 wt % DABAP. Intermediate values were measured for the other compounds.

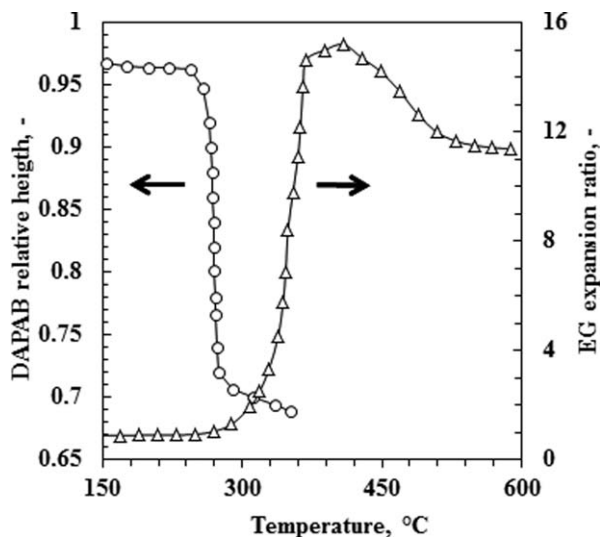


Figure 6. Thermomechanical characterization of the softening of DABAP and the exfoliation process of the expandable graphite (EG) in a nitrogen atmosphere. The temperature was scanned at rates of 4°C min^{-1} and $10^\circ\text{C min}^{-1}$, respectively. A penetration probe was used for the DABAP and a flat-tipped standard expansion probes was used for the EG. The applied force was 0.01 N for the DABAP and 0.02 N for the expandable graphite.

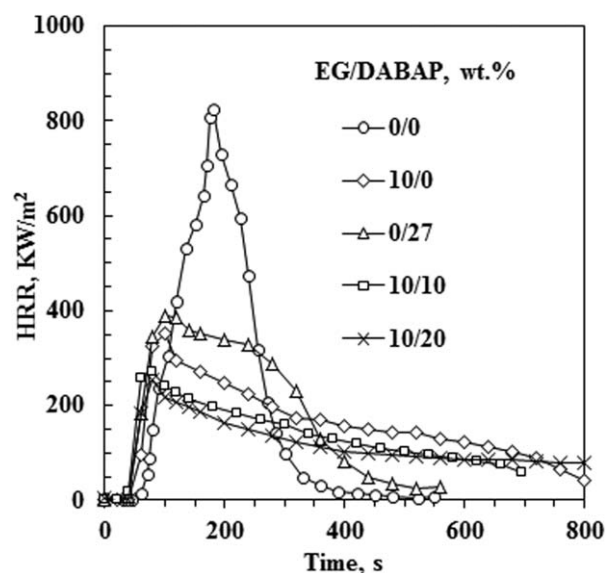


Figure 7. Cone calorimeter heat release rate curves for the polyethylene compounds with expandable graphite and DABAP. The sample sheets were backed by aluminium foil and their dimensions were $100 \times 100 \times 3.2 \text{ mm}$. They were mounted horizontally and exposed from above to an external heat flux of 35 kW m^{-2} .

All the neat samples ignited and flamed for extended periods of time. The heat release curves for the neat polyethylene compound exhibited the shape characteristic of a thermally thin sample.¹⁹ Thermally thin samples are identified by a sharp peak in their HRR curves as the whole sample is pyrolyzed at once. HRR curves characteristic of thermally thick, char-producing samples show a sudden rise to a plateau value.¹⁹ The HRR curves for the flame retarded samples approach this shape. They showed a rapid rise after ignition followed by a slower

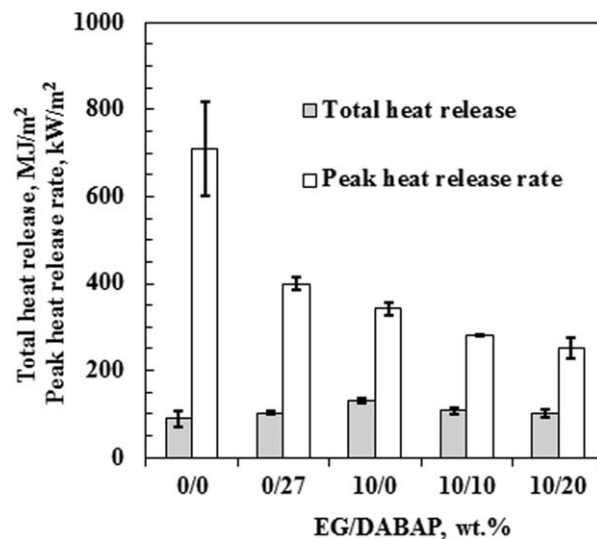


Figure 8. Cone calorimeter peak heat release rates and total heat release for the polyethylene compounds with expandable graphite and DABAP. The sample sheets were backed by aluminium foil and their dimensions were $100 \times 100 \times 3.2 \text{ mm}$. They were mounted horizontally and exposed from above to an external heat flux of 35 kW m^{-2} .

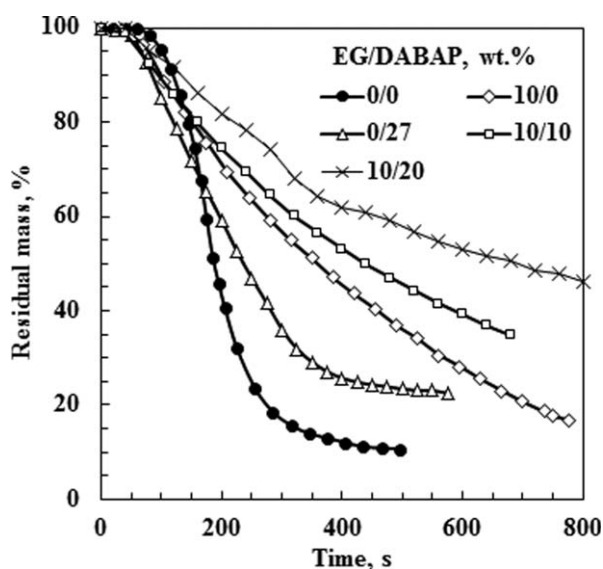


Figure 9. Cone calorimeter mass loss curves for the polyethylene compounds with expandable graphite and DABAP. The sample sheets were backed by aluminium foil and their dimensions were $100 \times 100 \times 3.2$ mm. They were mounted horizontally and exposed from above to an external heat flux of 35 kW m^{-2} .

downward taper. The HRR curve for the 27 wt % DABAP compound showed a third phase where a faster decay in the HRR occurred. All the flame retarded samples expanded during the fire test but expansion was more pronounced in the samples containing EG. Figure 8 shows the effect of adding both EG and DABAP on the pHRRs and the total heat release. The pHRR results are also tabulated in Table II. The pHRR for the neat polyethylene was $710 \pm 109 \text{ kW m}^{-2}$. The best result was

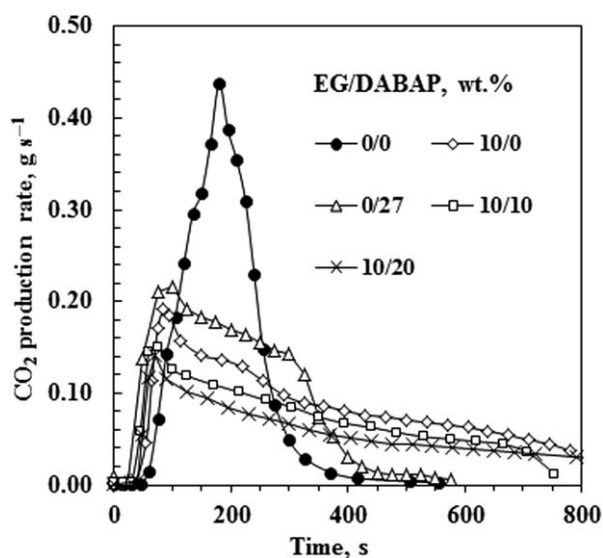


Figure 11. Cone calorimeter CO_2 production curves for the polyethylene compounds with expandable graphite and DABAP. The sample sheets were backed by aluminium foil and their dimensions were $100 \times 100 \times 3.2$ mm. They were mounted horizontally and exposed from above to an external heat flux of 35 kW m^{-2} .

obtained from 10 wt % EG plus 20 wt % DABAP ($252 \pm 24 \text{ kW m}^{-2}$) but even addition of 10 wt % EG alone reduced the value to $342 \pm 15 \text{ kW m}^{-2}$. Table II shows that the 10 wt % EG compound is more effective at reducing the pHRR than the 27 wt % DABAP compound. The improved fire performance with respect to the pHRR is attributed to the formation of a heat-insulating protective barrier at the solid surface. This limited heat transfer to the substrate and thus slowed down the rate of thermal degradation.

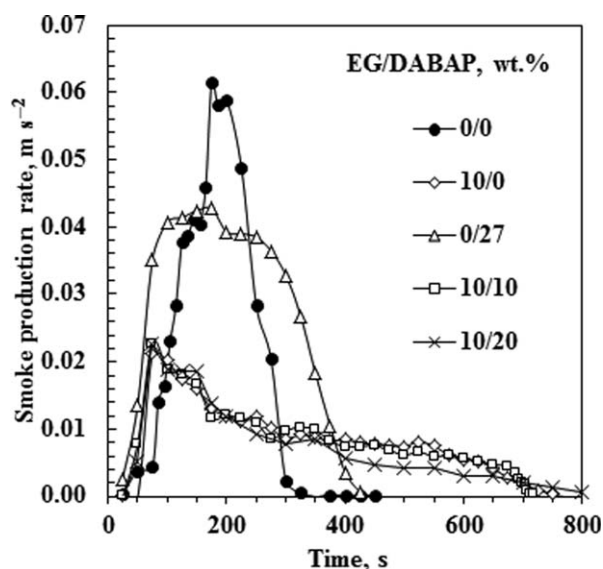


Figure 10. Cone calorimeter smoke production curves for the polyethylene compounds with expandable graphite and DABAP. The sample sheets were backed by aluminium foil and their dimensions were $100 \times 100 \times 3.2$ mm. They were mounted horizontally and exposed from above to an external heat flux of 35 kW m^{-2} .

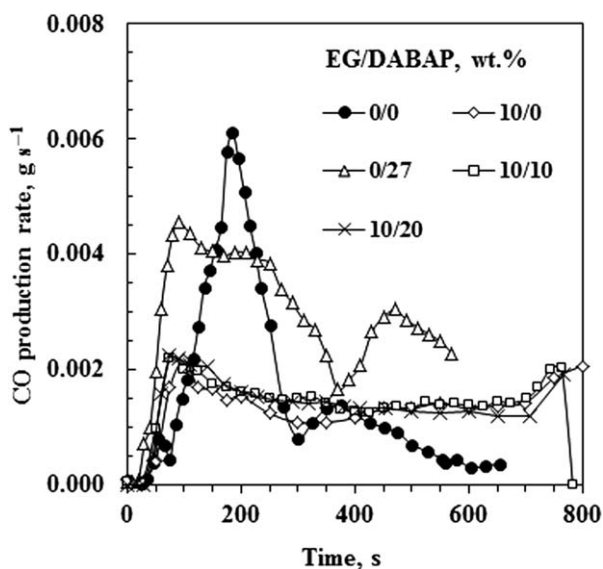


Figure 12. Cone calorimeter CO production curves for the polyethylene compounds with expandable graphite and DABAP. The sample sheets were backed by aluminium foil and their dimensions were $100 \times 100 \times 3.2$ mm. They were mounted horizontally and exposed from above to an external heat flux of 35 kW m^{-2} .

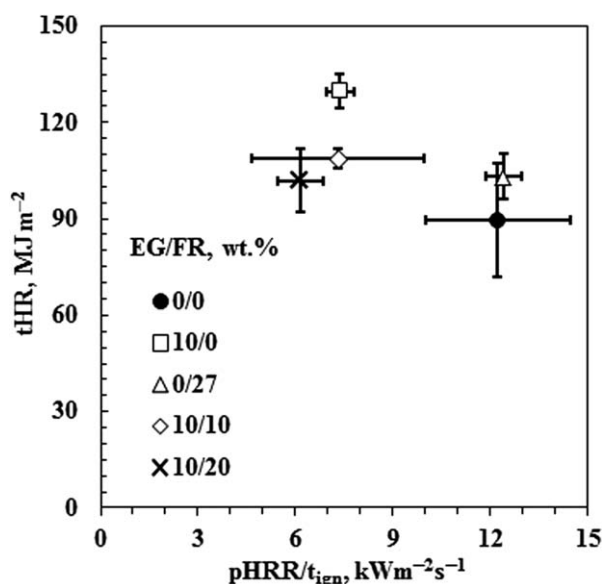


Figure 13. Petrella plot²¹ for the polyethylene compounds with expandable graphite and DABAP. The sample sheets were backed by aluminium foil and their dimensions were 100 × 100 × 3.2 mm. They were mounted horizontally and exposed from above to an external heat flux of 35 kW m⁻².

Figure 9 confirms that the addition of the EG reduced the mass loss rate (MLR). This can be attributed to the expansion of the intercalated graphite, which forms a low density layer of loose 'worm like' structures at the surface. Visual inspection of the residues showed that the DABAP containing compounds formed a denser charred foam layer at the polymer interface.

Table II lists the ignition and flame out times for the various samples. Addition of the flame retardants increased the propensity of the material to ignite. The time to ignition (t_{ign}) was 58 ± 3 s for the neat polyethylene and 46 ± 1 s for the compound containing 10 wt % EG but decreased to 33 ± 5 for the compound containing 27 wt % DABAP. The lower ignition times are tentatively attributed to rapid decomposition of the intumescent flame retardants occurring at a lower temperature than for the neat polymer. This means that more flammable volatiles are released at an earlier stage in sufficient quantities to allow ignition to occur.

Table II. Cone Calorimeter Data Summary

Property	Units	EG/DABAP, wt %				
		0/0	10/0	0/27	10/10	10/20
Time to ignition (t_{ign})	s	58 ± 3	46 ± 1	33 ± 5	39 ± 3	41 ± 1
Time to pHRR	S	177 ± 6	92 ± 3	105 ± 13	72 ± 6	75 ± 0
Time to flame out	s	773 ± 307	869 ± 68	537 ± 69	993 ± 46	1124 ± 106
Total heat release (tHR)	MJ m ⁻²	90 ± 18	130 ± 5	103 ± 3	109 ± 7	102 ± 10
Peak heat release rate (pHRR)	kW m ⁻²	710 ± 109	342 ± 15	400 ± 16	282 ± 3	252 ± 24
MAHRE	MJ m ⁻²	316 ± 47	199 ± 13	276 ± 12	168 ± 6	146 ± 7
FIGRA	kW m ⁻² s ⁻¹	4.01 ± 0.52	3.73 ± 0.09	3.86 ± 0.68	3.95 ± 0.37	3.36 ± 0.32
pHRR/ t_{ign}	kW m ⁻² s ⁻¹	12.2 ± 2.2	7.38 ± 0.41	12.4 ± 2.7	7.31 ± 0.55	6.15 ± 0.71

The time to flame out showed considerable variability. See Table II. It was 773 ± 307 for the neat polyethylene, reduced to 539 ± 69 for the 27 wt % DABAP compound and was longer than both these times for all other compounds.

Figure 10 compares the smoke production rates (SPR) of the composites with that for the neat polyethylene. All the compounds containing EG showed similar performance with a considerable reduction in smoke generation. Adding DABAP lowered the peak SPR but the total amount of smoke released was higher. A potential explanation is as follows. The rate of smoke reduction is reduced owing to the barrier properties of the char layer that forms on the surface. However, ultimately more smoke is released because the aromatic additive itself has a greater tendency to produce smoke than the aliphatic polymer matrix.

Figures 11 and 12 show the CO₂ and CO release rate curves. The observed trends for CO₂ mirror those observed for the HRR (Figure 7) almost perfectly. This is expected as the HRR correlates with the oxygen consumption and hence the rate of CO₂ production. The curves for CO are more complex especially in the case of the 27 wt % DABAP compound. The cause for this behavior is not currently understood but it could be related to the particular way DABAP decomposes under simulated fire scenarios. Although the peak rate of CO release was higher for the neat polyethylene, the total amount produced by the additive containing compounds seems to be higher. However this is not significant as the CO production rate was almost two orders of magnitude lower than that of CO₂.

The fire growth rate (FIGRA) and the maximum average rate of heat emission (MAHRE) are indices that may be used to interpret cone calorimeter data.^{19,20} The MARHE parameter is defined as the peak value of the cumulative heat emission divided by time.²⁰ It provides a measure of the propensity for fire development under real scale conditions.²⁰ The FIGRA is an estimator for the fire spread rate and size of the fire whereas the MARHE guesstimates the tendency of a fire to develop.²⁰ The FIGRA is determined as

$$\text{FIGRA} = \text{pHRR}/\text{time to pHRR} \quad (1)$$

Table II lists the FIGRA and MAHRE indices. A marked reduction of up to 50% relative to the neat polyethylene was observed

for the MAHRE measured for the 10 wt % EG – 20 wt % DABAP combination. The FIGRA values, although somewhat reduced, did not differ markedly from those of the neat polyethylene.

The parameters that are pertinent to fire hazards are the fire load and flame spread.¹⁹ The Petrella plot is an attempt to gauge the magnitude of the fire hazard posed.^{19,21} It is a plot of the total heat evolved tHR (as fire load) against pHRR/ t_{ig} (as a fire growth index). For a material to be effectively flame retarded both the fire load and the fire growth index should assume low values. Figure 13 shows a Petrella plot for the present formulations.

Except for the 27 wt % DABAP compound, all the other flame retarded compounds showed a decrease in the pHRR/ t_{ig} parameter but a slight increase in the heat load. The former performed slightly worse than the neat polyethylene according to both Petrella parameters. The reason for this is that the ignition time reduction was higher than the reduction in the pHRR. The overall heat load was also higher than that of the neat polyethylene.

CONCLUSIONS

The DABAP was obtained by a facile precipitation reaction. This compound has a relatively high thermal stability. It commences to soften and melt at 257°C and simultaneously decomposes with rapid mass loss up to about 17 wt % observed just above this temperature. This is attributed to a decarboxylation reaction that releases CO₂. The thermal decomposition proceeded stepwise at higher temperatures and resulted in a char yield at 900°C of about 27 wt %.

The flame retardant performance of this compound on its own, and in combination with a high thermal-stability EG, was evaluated by cone calorimetry. Polyethylene containing 5 wt % carbon-black was used as reference. Cone calorimeter results showed that adding 10 wt % EG lowered the pHRR of carbon black-pigmented polyethylene from 710 ± 109 to 342 ± 15 kW m⁻², while the compound containing 27 wt % of the intumescent and 3 wt % carbon-black lowered it to 400 ± 16 kW m⁻². Combinations of these two additives decreased the pHRR even further.

The intumescent additive reduced the flame out time from 773 ± 307 to 537 ± 69 s while all other samples containing EG increased it. On the other hand, the addition of the EG had a much greater effect on reducing smoke emission.

All present additives caused a marginal decrease in the FIGRA fire index. The 10 wt % EG 20 wt % intumescent combination caused a staggering reduction of 50% in the MAHRE value. The Petrella plot (Figure 13), an alternative measure of the flame

retarding ability of a compound, indicated only marginal performance differences between the formulations tested.

This work is based on research supported by the South African Research Chairs Initiative of the Department of Science and Technology (DST) and the National Research Foundation (NRF). Any opinion, findings, and conclusions or recommendations expressed in this material are those of the authors and therefore the NRF and DST do not accept any liability with regard thereto.

REFERENCES

1. Weil, E. D.; Levchik, S. V. *J. Fire Sci.* **2008**, *26*, 5.
2. Babrauskas, V.; Peacock, R. D. *Fire Safety J.* **1992**, *18*, 255.
3. Dasari, A.; Yu, Z. Z.; Cai, G. P.; Mai, Y. W. *Prog. Polym. Sci.* **2013**, *38*, 1357.
4. Qu, B.; Xie, R. *Polym. Int.* **2003**, *52*, 1415.
5. Xie, R.; Qu, B. *J. Appl. Polym. Sci.* **2001**, *80*, 1181.
6. Xie, R.; Qu, B. *J. Appl. Polym. Sci.* **2001**, *80*, 1190.
7. Pang, X. Y.; Song, M. *Adv. Mater. Res.* **2012**, *260–261*, 779.
8. Sun, Z.; Ma, Y.; Xu, Y.; Chen, X.; Chen, M.; Yu, J.; Hu, S.; Zhang, Z. *Polym. Eng. Sci.* **2013**, doi: 10.1002/pen.23659.
9. Han, Z.; Li, Y.; Zhao, H. Proc. IEEE Int. Conf. Properties and Applications of Dielectric Materials, **2007**, Article No. 4062794, pp. 828–831.
10. Camino, G.; Costa, L.; Martinasso, G. *Polym. Degrad. Stab.* **1989**, *23*, 359.
11. Wang, J. Q.; Chow, W. K. *J. Appl. Polym. Sci.* **2005**, *97*, 366.
12. Lewin, M. *J. Fire Sci.* **1999**, *17*, 3.
13. Furdin, G. *Fuel* **1998**, *77*, 479.
14. Camino, G.; Duquesne, S.; Delobel, R.; Eling, B.; Lindsay, C.; Roels, T. In *Fire and Polymers*; Nelson, G. L., Wilkie, C. A., Eds.; ACS Pub: Washington DC, **2001**; Chapter 8, p 90.
15. Wissler, M. *J. Power Sources* **2006**, *156*, 142.
16. Chung, D. D. L. *J. Mater. Sci.* **1987**, *22*, 4190.
17. Chung, D. D. L. *J. Mater. Sci.* **2002**, *37*, 1475.
18. Coates, J. In *Encyclopedia of Analytical Chemistry*; Meyers, R., Ed.; John Wiley & Sons Ltd, Chichester, **2000**, p 10815.
19. Schartel, B.; Hull, T. R. *Fire Mater.* **2007**, *31*, 327.
20. Sacristán, M.; Hull, T. R.; Stec, A. A.; Ronda, J. C.; Galià, M.; Cádiz, V. *Polym. Degrad. Stab.* **2010**, *95*, 1269.
21. Petrella, R. V. *J. Fire Sci.* **1994**, *12*, 14.